Electronic Supplementary Material (ESI) for Soft Matter.

Supporting Information: Effects of Impedance Measurement Frequency on Hybrid Response Pressure Sensors

Zhengjie Li[a], Kyoung-Ho Ha[b], Zheliang Wang[a], Sangjun Kim[b], Ben Davis[b], Ruojun Lu[b], Jayant Sirohi[a], and Nanshu Lu[a,b,c,d]

[a]*Department of Aerospace Engineering and Engineering Mechanics, the University of Texas at Austin, Austin, Texas 78712, United States*
[b]*Department of Mechanical Engineering, the University of Texas at Austin, Austin, Texas 78712, United States*
[c]*Department of Biomedical Engineering, the University of Texas at Austin, TX 78712, United States*
[d]*Department of Electrical and Computer Engineering, the University of Texas at Austin, TX 78712, United States*

October 28, 2022

1 PNC characterization

1.1 Frequency-dependent conductivity and relative permittivity

We adopted Eq. 1 and Eq. 3 in main text to fit the measured conductivity and relative permittivity of PNC, respectively. The corresponding fitting parameters are listed in Table S1 and the corresponding resistivity figure is shown in Fig. S1:

Table 1: Fitted parameters for PNC conductivity Eq. 1 and relative permittivity Eq. 3

Doping ratio (wt %)	σ_{dc}[S/m]	s	α	k_{air0dc}	p	β
0.25	5.0e-11	0.8021	3.43e-11	1.11	1.21	8.18
0.50	3.0e-8	0.7521	2.46e-10	1.30	1.31	28.12
0.75	1.4e-6	0.7038	1.12e-10	4.03	1.30	2.06e2
1.00	6.7e-6	0.5805	2.006e-10	4.39	1.42	2.11e3

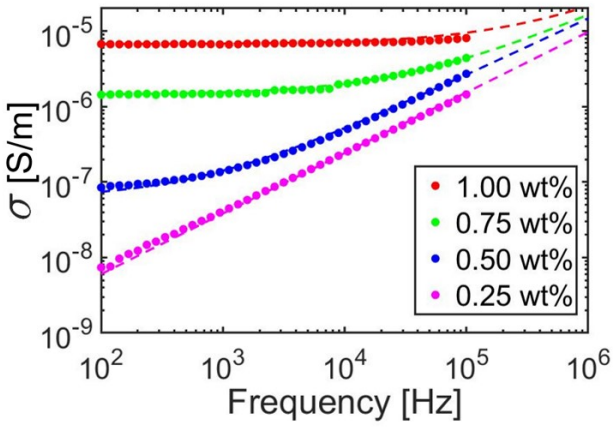

Fig. S 1: PNC conductivity vs. AC frequency with different CNT doping ratios: markers are experimentally measured and dashed lines are fitted using Eq. 1.

1.2 Validation of PNC air capacitance

Our equivalent circuit are built under four assumptions: 1) the electrical field is uniform and perpendicular to the parallel electrodes; 2) the PNC has a uniform porosity φ_0, and all the applied compression is accommodated by the reduction of porosity; 3) there is no lateral deformation when HRPS is subjected to pressure; 4) the frequency and pressure effects are fully decoupled. Based on the assumptions in the main text, we establish the analytical expression for C_{air} as a function of both the applied compressive strain e and the AC frequency ω:

$$C_{air}(e,\omega) = \frac{C_{air0}(\omega)\varphi_0}{(\varphi_0 - e)} \tag{S1}$$

In order to validate this theoretical expression, we adopted the experiment set up mentioned in main text section 2.2, 2.3, and Fig. 3a. The PNC was sandwiched between two electrodes and then connected to LCR meter (Keysight E4980AL). A Dynamic Mechanical Analyzer (DMA,RSA-G2, TA Instruments) was used to compress the PNC in its thickness direction. The PNC was under pressure at a fixed frequency. The measurements were taken in the parallel mode. The corresponding compressive strain e was converted from the displacement recorded by the DMA and C_p was recorded from the LCR meter. Because of the parallel mode, we have $C_p = C_{air}$.

We plot the experimental results as colored dots and the theoretical expression Eq. S1 as solid curves in Fig. S2. The theoretical results agree well with the theory for 0.25 wt%, 0.50 wt%, and 0.75 wt%. However, there is a big discrepancy between the two for 1.00 wt% PNC. This discrepancy might be a result of small resistance of 1.00 wt% PNC, which causes the electrical potential to decrease along the ligament of PNC and breaks the assumption of vertical electrical field [1]. Due to the difficulties in analytical modeling of capacitance change under distorted electrical field, we propose the following phenomenological form for the air capacitance C_{air}:

$$C_{air}(e,\omega) = \frac{C_{air0}(\varphi_0)^b}{(\varphi_0 - e)^b,} \tag{S2}$$

where b is a fitting parameter and the value used in this work is listed in Table. 2. The results are plotted as dashed curves in Fig. S2d and match well with the experiments.

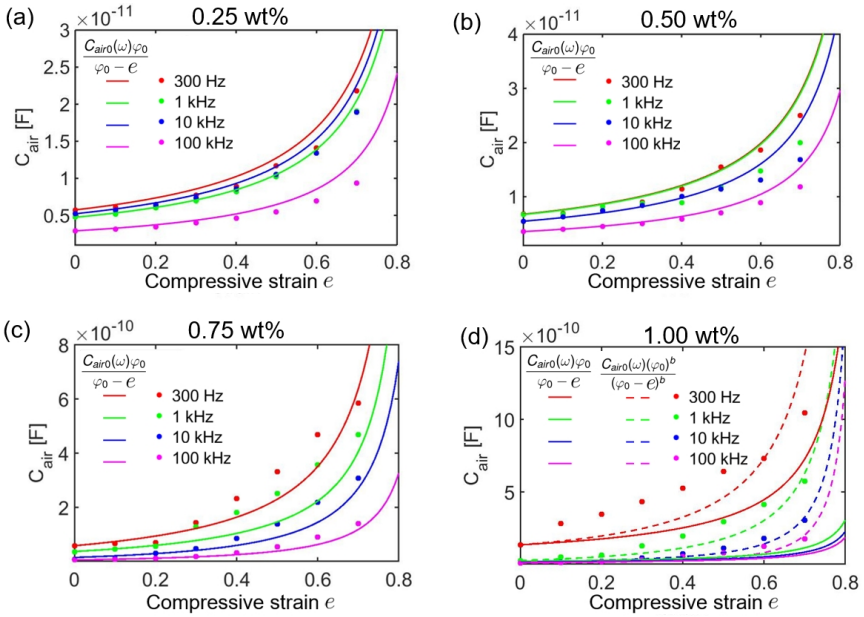

Fig. S 2: Theoretical (Eq. S1, solid curves), experimental (dots) and fitted (Eq. S2, dashed curves) PNC capacitance vs. compressive strain with the CNT doping ratios of (a) 0.25 wt%, (b) 0.5 wt%, (c) 0.75 wt%, and (d) 1 wt%.

Table 2: Fitting parameter b in Eq. of 1.00 wt% PNC at different frequencies

Frequency	b
100 kHz	1.88
10 kHz	1.72
1 kHz	1.55
300 Hz	1.41

2 Sensitivity of HRPS with different CNT doping ratios at different frequencies

The normalized capacitance pressure response $\frac{\triangle C}{C_0}$ vs P is plotted in Fig. S3. We replot the experimental results for C_{HRPS} in Section 2 by normalizing it by its initial capacitance C_0. According to the indication from the master curve, the performance of a HRPS with relatively large doping ratio can be optimized by using a relatively large measurement frequency. As shown in Fig. S3, for 0.25, 0.50, 0.75 wt% PNC, 300 Hz is the optimum frequency as its shows the largest normalized change of capacitance $\frac{\triangle C}{C_0}$. For 1.00 wt%, the optimum frequency is 10 kHz. This difference in the optimum frequency verifies our prediction and indication.

3 Piezoresistive vs. piezocapacitive contributions

In the main text, the optimal frequency observed from Fig. 4c-e is one that keeps the two current fractions closest to 0.5, the ones with the most balanced hybrid response. To explain this phenomena, we rewrite the expression of C_{HRPS}/C_i and express it with C_{air}, C_i and $Y = \omega R C_{air}$:

$$\frac{C_{HRPS}}{C_i} = \frac{1+\omega^2 R^2 C_{air}^2}{1+\omega^2 R^2 C_{air}^2 + \omega^2 R^2 C_i C_{air}} = \frac{1+Y^2}{1+Y^2+Y^2\frac{C_i}{C_{air}}} = \frac{1}{1+\frac{Y^2}{1+Y^2}\frac{C_i}{C_{air}}} \tag{S3}$$

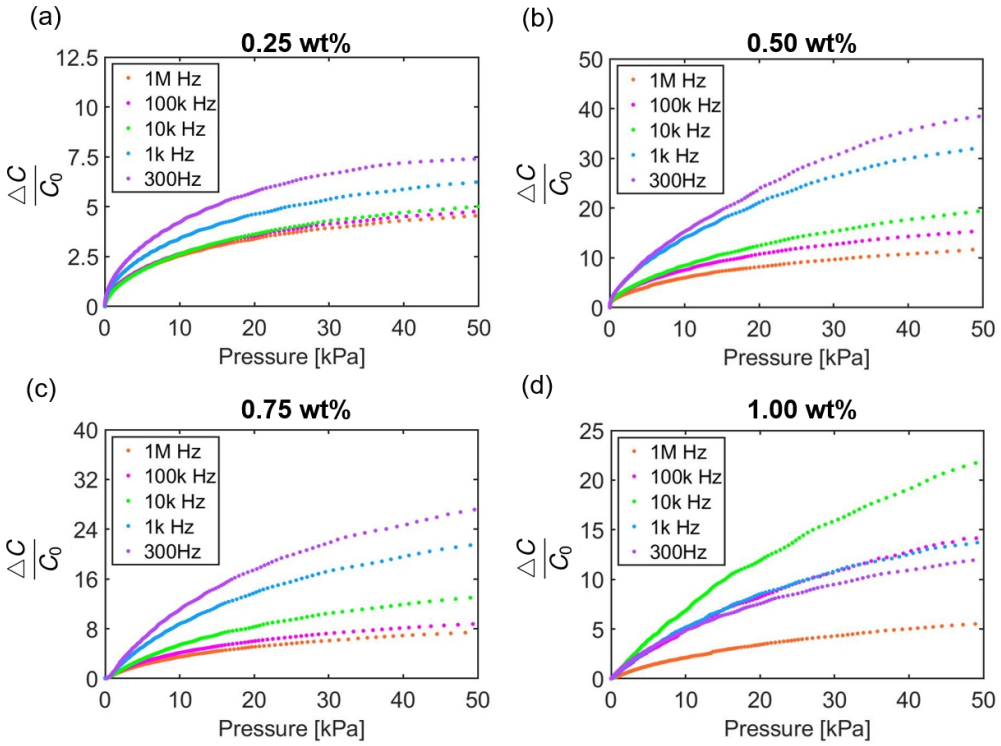

Fig. S 3: The normalized capacitance vs. pressure of HRPS with different doping ratios at different frequencies. It is clear that 300 Hz offers the best sensitivity for 0.25 wt%, 0.5 wt%, and 0.75 wt% HRPS whereas it is 10 kHz for 1 wt% HRPS.

We further note that $Y = 1$ means the current flowing through the resistive branch equals to current flowing through the capacitive branch (Current fraction = 0.5). Here, we define the e_0 as the strain of the undeformed state, and the corresponding capacitance of HRPS as C_{HRPS0}, air capacitance as C_{air0} and $Y_0 = \omega R_0 C_{air0}$. Similarly, we can define e_1 as the strain of the deformed state after compression, and the corresponding capacitance of HRPS as C_{HRPS1} air capacitance as C_{air1} and $Y_1 = \omega R(e_1) C_{air}(e_1)$. Therefore, we have:

$$\frac{C_{HRPS1}}{C_{HRPS0}} = \frac{1 + \frac{Y_0^2}{1+Y_0^2}\frac{C_i}{C_{air0}}}{1 + \frac{Y_1^2}{1+Y_1^2}\frac{C_i}{C_{air1}}} \tag{S4}$$

$\frac{C_{HRPS1}}{C_{HRPS0}}$ is the normalized sensor capacitance after deformation and directly reflects the sensor sensitivity via $\frac{C_{HRPS1}}{C_{HRPS0}} = 1 + \frac{\Delta C_{\epsilon=\epsilon_1}}{C_0}$. The larger $\frac{C_{HRPS1}}{C_{HRPS0}}$, the better the sensitivity of HRPS.

The compression is performed at the same measuring frequency. Therefore, we note that $R_0(\omega)$,$C_{air0}(\omega)$ is unchanged during compression:

$$R(e,\omega) = \frac{R_0(\omega)}{\varphi_0^2}(e-\varphi_0)^2 + \frac{R_0(\omega)}{1000},\ C_{air}(e,\omega) = \frac{C_{air0}(\omega)\varphi_0}{(\varphi_0 - e)} \tag{S5}$$

Then we write Y_1/Y_0:

$$\frac{Y_1}{Y_0} = \frac{\omega R(e_1,\omega) C_{air}(e_1,\omega)}{\omega R(e_0,\omega) C_{air}(e_0,\omega)} = \frac{(\frac{1}{\varphi_0^2}(e_1-\varphi_0)^2 + \frac{1}{1000})\frac{\varphi_0}{(\varphi_0-e_1)}}{(\frac{1}{\varphi_0^2}(e_0-\varphi_0)^2 + \frac{1}{1000})\frac{\varphi_0}{(\varphi_0-e_0)}} \tag{S6}$$

Let strain ϵ_0=0, ϵ_1=0.7, we get $Y_1 = 0.1912 Y_0$ from equation (S6), $C_{air0} = 5.375 C_{air1}$ from equation

(S5). Therefore, the equation (S4) can be expressed as

$$\frac{C_{HRPS1}}{C_{HRPS0}} = \frac{1 + \frac{Y_0^2}{1+Y_0^2}\frac{C_i}{C_{air0}(\omega)}}{1 + \frac{(0.1912Y_0)^2}{1+(0.1912Y_0)^2}\frac{5.375C_i}{C_{air0}(\omega)}} \tag{S7}$$

Eq. (S7) suggests that the initial Y_0 can determine the change of normalzied capacitance C_{HRPS1}/C_{HRPS0} during compression. Eq. (S7) is plotted as solid curves in Fig. S4. The markers represent the Y_0 values from the experiment in Fig. 6 and its corresponding normalized capacitance changes.

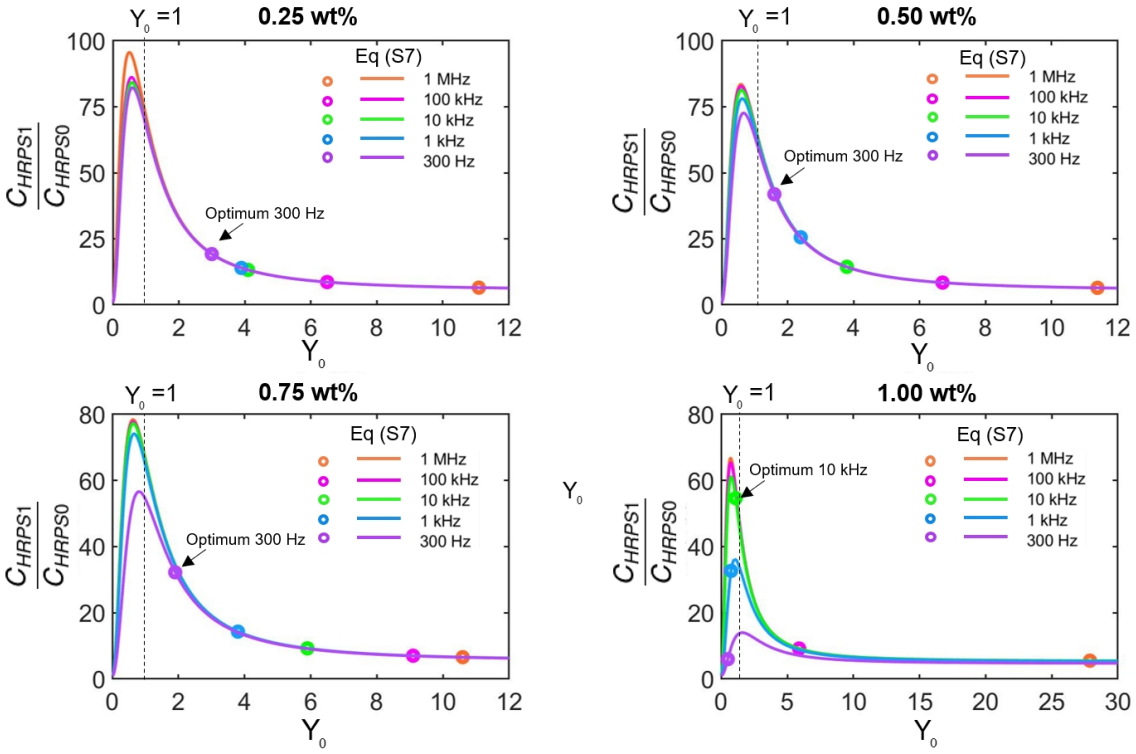

Fig. S 4: Frequency conductivity response of PNC with different doping ratio.

Fig. S4 shows that the normalized capacitance change, which is equivalent to sensitivity, first increase and then decrease with increasing Y_0. For all cases investigated, the peak of sensitivity is near $Y_0 = 1$, which echoes with our finding that an initial balanced hybrid response results in a better sensitivity.

References

[1] Kyoung-Ho Ha, Weiyi Zhang, Hongwoo Jang, Seungmin Kang, Liu Wang, Philip Tan, Hochul Hwang, and Nanshu Lu. Highly sensitive capacitive pressure sensors over a wide pressure range enabled by the hybrid responses of a highly porous nanocomposite. *Advanced Materials*, 33(48):2103320, 2021.